Received: 22 April 2020 | Accepted: 15 May 2020
DOI: 10.1002/hyp.13825

HPEYE

WILEY

Groundwater–surface water exchange in the intertidal zone detected by hydrologic and coastal oceanographic measurements

James W. Heiss[1] | Holly A. Michael[2,3] | Jack Puleo[3]

[1]Department of Environmental, Earth and Atmospheric Sciences, University of Massachusetts Lowell, Lowell, Massachusetts, USA

[2]Department of Earth Sciences, University of Delaware, Newark, Delaware, USA

[3]Department of Civil and Environmental Engineering, University of Delaware, Newark, Delaware, USA

Correspondence
James W. Heiss, Department of Environmental, Earth and Atmospheric Sciences, University of Massachusetts Lowell, Lowell, MA.
Email: james_heiss@uml.edu

Funding information
National Science Foundation, Grant/Award Number: EAR-1246554

1 | INTRODUCTION

This study demonstrates the use of coupled surface water and subsurface hydrologic measurements to characterize groundwater–surface water exchange across the intertidal zone of a micro-tidal high energy sandy beach. Water content and saturated pore pressure measurements are combined with waterline time series extracted from thermal and visible-band (RGB) imagery to produce a continuous 8-hr (real time) animation of the interaction between waves, tides, and unsaturated groundwater dynamics.

2 | DESCRIPTION

The exchange of groundwater and surface water across the intertidal zone of sandy beaches transports salt (Robinson et al., 2017), chemicals (Santos et al., 2008), heat (Befus, Cardenas, Erler, Santos, & Eyre, 2013), and biota (Adyasari, Hassenrück, Oehler, Sabdaningsih, & Moosdorf, 2019; Gast, Elgar, & Raubenheimer, 2015), and alters sediment transport processes (Bakhtyar, Brovelli, Barry, & Li, 2011; Corvaro, Miozzi, Postacchini, Mancinelli, & Brocchini, 2014, Karambas, 2003). Chemical fluxes associated with fluid exchange at the land–sea interface can reduce species diversity (Amato et al., 2016), lead to seagrass loss (Valiela et al., 1997), and impair coastal water quality (Paerl, 1997). A number of field, laboratory, and modelling studies have investigated groundwater–surface water interactions in the swash zone driven by waves and tides (e.g. Heiss, Ullman, & Michael, 2014; Sous, Lambert, Rey, & Michallet, 2013; Sous, Petitjean, & Rey, 2016; Turner & Masselink, 1998; Xin, Robinson, Li, Barry, & Bakhtyar, 2010). Laboratory studies show that a groundwater circulation pattern forms under the swash zone due to infiltration in the upper swash zone and discharge in the lower swash (Sous et al., 2013; Sous, Lambert, Michallet, & Rey, 2011; Turner, Rau, Austin, & Andersen, 2016). Sous et al. (2016) first observed the swash zone circulation cell in the field and characterized its temporal and spatial variability in response to overlying swash zone forcing using pore pressure measurements and LiDAR. The results showed that the infiltration and discharge zones, corresponding to the landward and seaward sides of the circulation cell, shifted seaward with the swash zone during a falling tide, indicating that the infiltration and discharge zones across the lower saturated beach face are dynamic in response to swash and tidal forcing. While a number of the above studies (e.g. Sous et al., 2011, 2013, 2016; Turner et al., 2016) provide a comprehensive description of saturated groundwater dynamics under the swash zone, fewer studies have focused on flow in the unsaturated zone. Steenhauer, Pokrajac, O'Donoghue, and Kikkert (2011) used digital imagery and pore pressure measurements to monitor the downward movement of the air/water interface in a laboratory beach. However, saturation dynamics within and across the unsaturated region of the swash zone are less understood. With the large quantity of seawater that can infiltrate into the unsaturated zone from wave swash (Heiss, Puleo, Ullman, & Michael, 2015), saturation dynamics are likely to affect sediment transport processes and the availability of reactive particles in seawater that contribute to biogeochemical transformations in the beach aquifer.

Energetic wave conditions and the disparate time scales of tides, waves, and swash on beaches present a challenge when seeking to understand coupled dynamics between surface and subsurface flow.

As a result, combined groundwater and surface water field measurements are scarce on beaches with waves (e.g. Sous et al., 2016), but are needed to link subsurface flow and solute transport processes to tidal and swash zone forcing. Previous studies have provided snapshots of moisture content and swash and groundwater levels using subsurface and surface measurements (e.g. Heiss et al., 2015). However, measurement snapshots can mask processes with time scales shorter than the snapshot interval. This under sampling leads to the inability to fully understand dynamics between typical events of interest (e.g. swash events) and uncertainty in the range of timescales of groundwater–surface water interactions.

In this study, high-frequency synchronous surface and subsurface measurements on a beach with waves were collected using multiple sensors and video imagery types to create an uninterrupted visualization of groundwater flow processes and overlying tide and swash motion. The study site was located on Cape Henlopen, Delaware, USA, a sandy spit at the mouth of the Delaware Bay. A suite of instruments was deployed at Herring Point (38°45′51.8″N, 75°04′54.0″W) on the ocean side of Cape Henlopen where the tidal range is 1.41 m (NOAA tidal station 8557830, Lewes, Delaware). The inner surf-zone-significant wave height was 0.57 m and the hydraulic conductivity of the intertidal sediment was 21 m/d.

Moisture sensors and pressure transducers were installed in a 2.5-m wide cross-shore transect 3 m landward of the high tide line. In the initially unsaturated zone of the upper beach face, 31 Meter Environmental EC-5 soil moisture sensors were mounted to six instrument arrays distributed across the transect, with 5–6 moisture sensors per array (2–18 cm depth). A GE Druck PTX 1835 pressure transducer was placed at the bottom of each array (1.1 m depth) to monitor water table response to unsaturated swash infiltration. The measured water table elevation was extended to the beach face to estimate the water table–beach face intersection (i.e. exit point). Groundwater discharges from the beach seaward of the exit point at this site (Heiss et al., 2015). The moisture sensors and pressure transducers were wired to two Campbell Scientific CR1000 data loggers that logged at 5 and 16 Hz, respectively.

Two video imagers tracked surface water features. A Sony DFW-X710 RGB imager (1,024 × 768 pixels) was used to identify the leading edge of the swash lens (hereafter referred to the swash edge) at 4 Hz and a thermal FLIR systems SC645 imager (640 × 480 pixels) recording at 3.125 Hz was used to locate the boundary between the saturated and unsaturated beach face (hereafter referred to as the surface saturation boundary). The location of the surface saturation boundary was identifiable in the thermal images due to the temperature contrast between the colder lower saturated beach face and the warmer upper unsaturated beach face. Images were recorded from an elevation of 6 m on a metal tower located 20 m offset from the instrument transect in the alongshore direction. Time series of the cross-shore position of the swash edge and surface saturation boundary were extracted from timestack images of a pixel transect at approximately the same cross-shore location as the instrument transect. Timestack images depict pixel intensity of each frame in a sequence of images at a single cross-shore location (Aagaard & Holm, 1989). All images were georectified using ground control points surveyed using an RTK-GPS. Additional details of the instrumentation can be found in Heiss et al. (2015).

On June 27, 2013, sensors and imagers began recording during a rising tide when the swash zone was still seaward of the instrument array. All sensors and imagers were time synchronized using a shared Garmin GPS antenna and data timestamps were zeroed to the start of the experiment. The swash edge, tidal water line, moisture content, and water table elevation were monitored over a tidal cycle, spanning the approach of the swash zone to the dry upper beach face, full saturation, and swash zone retreat during ebb tide.

Animation S1 shows a 7.8 hr (real time) animation of the coupled dynamics between saturation and overlying tide and swash forcing. The bottom panel shows the cross-shore position of the tidal water line (blue) and the swash edge (black line) relative to the most landward sensor array (y = 0 m). The animation illustrates the role of swash infiltration on saturating the beach during a rising tide. As the tide level migrated landward, individual swash events progressively introduced more seawater into the unsaturated zone. The animation shows that the position of the most landward fully saturated cross section (i.e. most shoreward location where the saturated zone joins the beach surface; Steenhauer et al. (2011)) contacted the farthest seaward array at 6,620 s when the tide level was 2.0 m seaward, indicating that the beach aquifer was in direct connection with the subaerial beach face. This area of the beach face represents an important region where infiltrating solutes and biota in seawater bypass the unsaturated zone and immediately mix with underlying saturated pore water in the larger beach groundwater system. The farthest landward connection point between the saturated beach and the sand surface moved landward and seaward at approximately the same rate as the rise and fall of the tide. Seawater infiltrated into the unsaturated zone landward of this point when swash lenses inundated the dry beach face, while groundwater discharged from the beach seaward of the water table–beach face intersection (Heiss et al., 2015). Thus, the measurements show the change in aquifer storage resulting from unsaturated swash infiltration and demonstrate how infiltration and discharge zones can be tracked across the beach surface.

Animation S2 (Figure 1, snapshot) shows saturation and water table dynamics between individual swash events. The lens of infiltrating seawater was relatively unchanged in shape between swash events, but expanded vertically downward and horizontally landward when large swash events inundated the upper beach face. Moderate draining from the unsaturated zone was evident during longer periods when there was no swash inundation over the transect (e.g. 945–1,065 s), suggesting that infragravity waves may affect saturation dynamics in the unsaturated zone.

Hydrologic and coastal oceanographic measurements were combined in a novel experiment to reveal the variety of time scales of groundwater–surface water exchange and saturation dynamics in the swash zone of a sandy beach. The visualizations highlight the role of tides and swash processes on saturation characteristics of beach sediments and provide a more complete understanding of intertidal fluid exchange that can be overlooked using traditional snapshots of

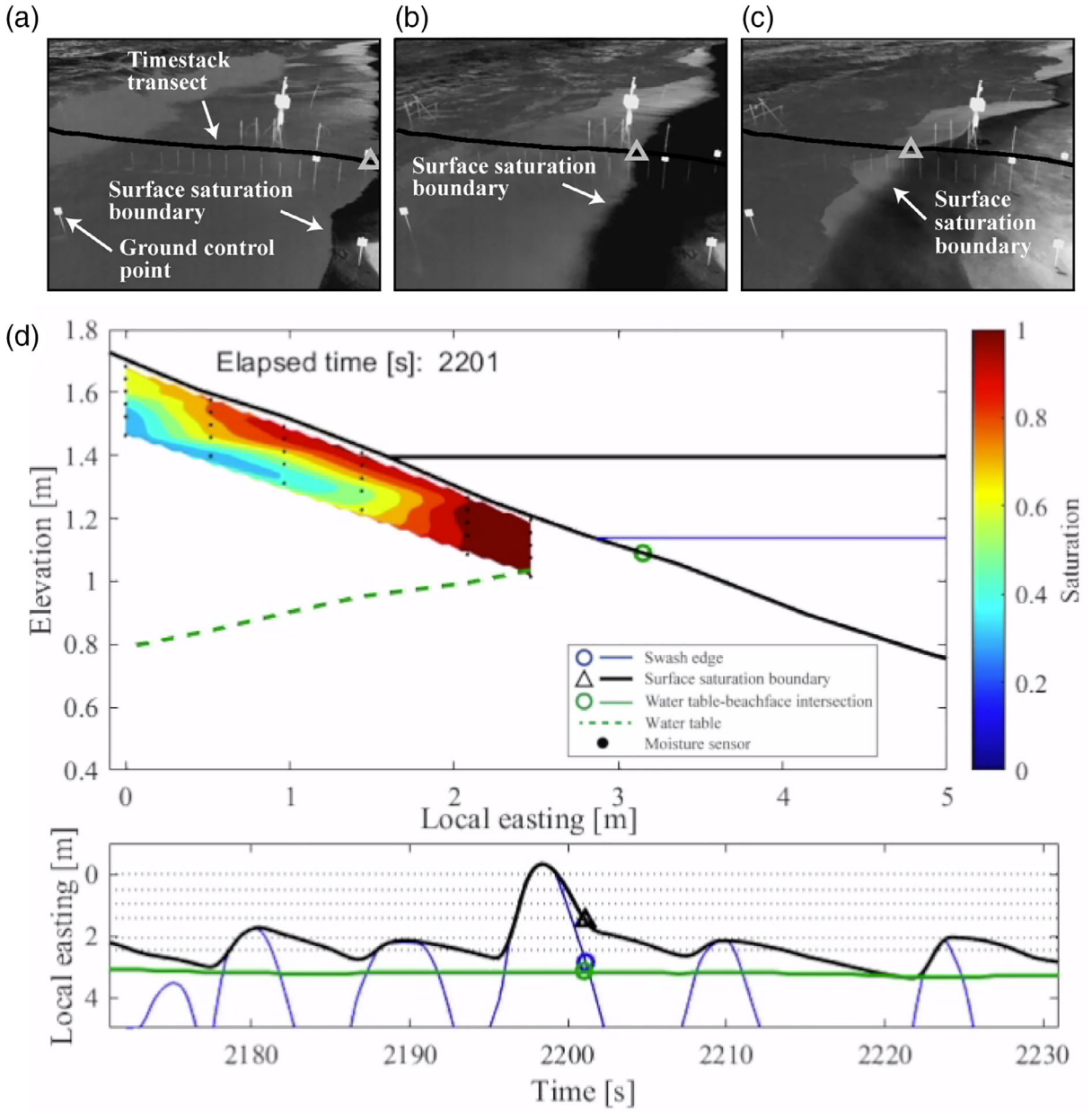

FIGURE 1 Thermal imagery and cross-section of surface and subsurface measurements. (a–c) Example seaward movement of the saturation boundary over a 4 s time period. The gray triangle in each frame shows the captured saturation boundary along the pixel transect. (d) Sediment moisture content below a swash lens during rising tide

hydrological processes. The findings demonstrate that integration of measurement approaches across disciplines is key to resolve otherwise undetected hydrological connections in these complex and energetic environments.

ACKNOWLEDGEMENTS

We thank University of Delaware faculty, graduate students, and undergraduate students Thomas McKenna, Aline Pieterse, Thijs Lanckriet, Adam Dejean, Veronica Citerone, Hannah Billian, Jillian McKenna, Nathan Veale, and Christopher Russoniello for assistance in the field. We also thank two anonymous reviewers for their helpful suggestions that improved the manuscript. This research was supported by National Science Foundation (NSF) grant EAR-1246554 to HM.

ORCID

James W. Heiss https://orcid.org/0000-0003-4246-624X

REFERENCES

Aagaard, T., & Holm, J. (1989). Digitization of wave run-up using video records. *Journal of Coastal Research*, *5*(3), 547–551.

Adyasari, D., Hassenrück, C., Oehler, T., Sabdaningsih, A., & Moosdorf, N. (2019). Microbial community structure associated with submarine groundwater discharge in northern Java (Indonesia). *Science of the*

Total Environment, *689*, 590–601. https://doi.org/10.1016/j.scitotenv.2019.06.193

Amato, D. W., Bishop, J. M., Glenn, C. R., Dulai, H., & Smith, C. M. (2016). Impact of submarine groundwater discharge on marine water quality and reef biota of maui. *Plos One*, *11*(11), e0165825. https://doi.org/10.1371/journal.pone.0165825.

Bakhtyar, R., Brovelli, A., Barry, D. A., & Li, L. (2011). Wave-induced water table fluctuations, sediment transport and beach profile change: Modeling and comparison with large-scale laboratory experiments. *Coastal Engineering*, *58*(1), 103–118. https://doi.org/10.1016/j.coastaleng.2010.08.004

Befus, K. M., Cardenas, M. B., Erler, D. V., Santos, I. R., & Eyre, B. D. (2013). Heat transport dynamics at a sandy intertidal zone. *Water Resources Research*, *49*(6), 3770–3786. https://doi.org/10.1002/wrcr.20325

Corvaro, S., Miozzi, M., Postacchini, M., Mancinelli, A., & Brocchini, M. (2014). Fluid-particle interaction and generation of coherent structures over permeable beds: An experimental analysis. *Advances in Water Resources*, *72*, 97–109. https://doi.org/10.1016/j.advwatres.2014.05.015

Gast, R. J., Elgar, S., & Raubenheimer, B. (2015). Observations of transport of bacterial-like microspheres through beach sand. *Continental Shelf Research*, *97*, 1–6. https://doi.org/10.1016/j.csr.2015.01.010

Heiss, J. W., Puleo, J. A., Ullman, W. J., & Michael, H. A. (2015). Coupled surface-subsurface hydrologic measurements reveal infiltration, recharge, and discharge dynamics across the swash zone of a sandy beach. *Water Resources Research*, *51*(11), 8834–8853. https://doi.org/10.1002/2015WR017395

Heiss, J. W., Ullman, W. J., & Michael, H. A. (2014). Swash zone moisture dynamics and unsaturated infiltration in two sandy beach aquifers. *Estuarine, Coastal and Shelf Science*, *143*, 20–31. https://doi.org/10.1016/j.ecss.2014.03.015

Karambas, T. V. (2003). Modelling of infiltration-exfiltration effects of cross-shore sediment transport in the swash zone. *Coastal Engineering*, *45*(1), 63–82. https://doi.org/10.1142/S057856340300066X

Paerl, H. W. (1997). Coastal eutrophication and harmful algal blooms: Importance of atmospheric deposition and groundwater as new nitrogen and other nutrient sources. *Limnology and Oceanography*, *42*(5_part_2), 1154–1165. https://doi.org/10.4319/lo.1997.42.5_part_2.1154

Robinson, C., Xin, P., Santos, I. R., Charette, M. A., Li, L., & Barry, D. A. (2017). Groundwater dynamics in subterranean estuaries of coastal unconfined aquifers: Controls on submarine groundwater discharge and chemical inputs to the ocean. *Advances in Water Resources*, *115*, 315–331. https://doi.org/10.1016/j.advwatres.2017.10.041

Santos, I. R., Burnett, W. C., Chanton, J., Mwashote, B. M., Suryaputra, I. G. N. A., & Dittmar, T. (2008). Nutrient biogeochemistry in a Gulf of Mexico subterranean estuary and groundwater-derived fluxes to the coastal ocean. *Limnology and Oceanography*, *53*(2), 705–718. https://doi.org/10.4319/lo.2008.53.2.0705

Sous, D., Lambert, A., Michallet, H., & Rey, V. (2011). Groundwater pressure dynamics in a laboratory swash zone. *Journal of Coastal Research*, *64*, 2074–2078.

Sous, D., Lambert, A., Rey, V., & Michallet, H. (2013). Swash–groundwater dynamics in a sandy beach laboratory experiment. *Coastal Engineering*, *80*(2013), 122–136. https://doi.org/10.1016/j.coastaleng.2013.05.006

Sous, D., Petitjean, L., & Rey, V. (2016). Field evidence of swash groundwater circulation in the microtidal Rousty beach, France. *Advances in Water Resources*, *97*, 144–155. https://doi.org/10.1016/j.advwatres.2016.09.009

Steenhauer, K., Pokrajac, D., O'Donoghue, T., & Kikkert, G. A. (2011). Subsurface processes generated by bore-driven swash on coarse-grained beaches. *Journal of Geophysical Research*, *116*(C4), 1–17. https://doi.org/10.1029/2010JC006789

Turner, I. L., & Masselink, G. (1998). Swash infiltration-exfiltration and sediment transport. *Journal of Geophysical Research*, *103*(C13), 813–824.

Turner, I. L., Rau, G. C., Austin, M. J., & Andersen, M. S. (2016). Groundwater fluxes and flow paths within coastal barriers: Observations from a large-scale laboratory experiment (BARDEX II). *Coastal Engineering*, *113*, 104–116. https://doi.org/10.1016/j.coastaleng.2015.08.004

Valiela, I., McClelland, J., Hauxwell, J., Behr, P. J., Hersh, D., & Foreman, K. (1997). Macroalgal blooms in shallow estuaries: Controls and ecophysiological and ecosystem consequences. *Limnology and Oceanography*, *42*, 1105–1118. https://doi.org/10.4319/lo.1997.42.5_part_2.1105

Xin, P., Robinson, C., Li, L., Barry, D. A., & Bakhtyar, R. (2010). Effects of wave forcing on a subterranean estuary. *Water Resources Research*, *46*(W12505), 1–17. https://doi.org/10.1029/2010WR009632

SUPPORTING INFORMATION

Additional supporting information may be found online in the Supporting Information section at the end of this article.

How to cite this article: Heiss JW, Michael HA, Puleo J. Groundwater–surface water exchange in the intertidal zone detected by hydrologic and coastal oceanographic measurements. *Hydrological Processes*. 2020;1–4. https://doi.org/10.1002/hyp.13825